Research Article | Vol. 25, No. 16 | 7 Aug 2017 | OPTICS EXPRESS 19529
Optics EXPRESS

Investigation of bandwidth loading in optical fibre transmission using amplified spontaneous emission noise

DANIEL J. ELSON,* GABRIEL SAAVEDRA, KAI SHI, DANIEL SEMRAU, LIDIA GALDINO, ROBERT KILLEY, BENN C. THOMSEN AND POLINA BAYVEL

Optical Networks Group, Dept. of Electronic & Electrical Engineering, UCL, Torrington Place, London WC1E 7JE, UK

*uceedel@ucl.ac.uk

Abstract: The use of spectrally shaped amplified spontaneous emission noise (SS-ASE) as a method for emulating interfering channels in optical fibre transmission systems has been studied. It is shown that the use of SS-ASE leads to a slightly pessimistic performance relative to the use of conventionally modulated interfering channels in the nonlinear regime. The additional nonlinear interference noise (on the channel under test), due to the Gaussian nature of SS-ASE, has been calculated using a combination of the Gaussian noise (GN) and enhanced GN (EGN) models for the entire C-band (4.5 THz) and experimentally shown to provide a lower bound for transmission performance.

OCIS codes: (060.2330) Fiber optics communications; (060.2430) Fibers, single-mode.

References and links

1. R. Maher, A. Alvarado, D. Lavery, and P. Bayvel, "Increasing the information rates of optical communications via coded modulation: a study of transceiver performance," Sci. Rep. **6**, 21278 (2016).
2. R. Maher, T. Xu, L. Galdino, M. Sato, A. Alvarado, K. Shi, S. J. Savory, B. C. Thomsen, R. I. Killey and P. Bayvel, "Spectrally shaped DP-16QAM super-channel transmission with multi-channel digital back-propagation," Sci. Rep. **5**, 8214 (2015).
3. D. S. Millar, L. Galdino, R. Maher, M. Pajovic, T. Koike-Akino, G. Saavedra, D. J. Elson, D. Lavery, K. Shi, M. S. Erklinç, E. Sillekens, R. I. Killey, B. C. Thomsen, K. Kojima, K. Parsons, P. Bayvel, "A simplified dual-carrier DP-64QAM 1 Tb/s transceiver," in Proc. of Optical Fiber Communication Conference (OFC), M3D.2 (2017).
4. M. E. McCarthy, N. M. Suibhne, S.T Le, P. Harper and A. D. Ellis, "High spectral efficiency transmission emulation for non-linear transmission performance estimation for high order modulation formats," in Proc. of European Conference on Optical Communications (ECOC), P.5.7 (2014).
5. D. J. Elson, L. Galdino, R, Maher, R. I. Killey, B. C. Thomsen, and P. Bayvel,"High spectral density transmission emulation using amplified spontaneous emission noise," Opt. Lett. **41**(1), 68–71 (2016).
6. H. Zhang, H. G. Batshon, C. R. Davidson, D. Foursa and A. Pilipetskii, "Multi-dimensional coded modulation in long-haul fiber optic transmission," J. Lightwave Technol. **33**(13), 2876–2883 (2015).
7. L. Galdino, D. Semrau, D. Lavery, G. Saavedra, C. B. Czegledi, E. Agrell, R. I. Killey and P. Bayvel, "On the limits of digital back-propagation in the presence of transceiver noise," Opt. Express **25**(4), 4564–4578 (2017).
8. J. Cho, X. Chen, S. Chandrasekhar, G. Raybon, R. Dar, L. Schmalen, E. Burrows and A. Adamiecki, "Trans-atlantic field trial using probabilistically shaped 64-QAM at high spectral efficiencies and single-carrier real-time 250-Gb/s 16-QAM," in Proc. of Optical Fiber Communication Conference (OFC), Th5B.3 (2017).
9. G. Saavedra, M. Tan, D. J. Elson, L. Galdino, D. Semrau, Md. A. Iqbal, I.D. Phillips, P. Harper, N. Mac Suibhne, A. D. Ellis, D. Lavery, B. C. Thomsen, R. I. Killey, P. Bayvel, "Experimental demonstration of nonlinear distortions in ultra-wideband transmission systems," in Proc. of Optical Fiber Communication Conference (OFC), W1G.1 (2017).
10. P. Poggiolini, G. Bosco, A. Carena, V. Curri, Y. Jiang, and F. Forghieri, "The GN-model of fiber non-linear propagation and its applications," J. Lightwave Technol, **32**(4), 694-721 (2014).
11. A. Mecozzi and R. Essiambre, "Nonlinear shannon limit in pseudolinear coherent systems," J. Lightwave Technol, **30**(12), 2011-2024 (2012).

#293333 https://doi.org/10.1364/OE.25.019529
Journal © 2017 Received 27 Apr 2017; revised 14 Jul 2017; accepted 14 Jul 2017; published 4 Aug 2017

Optics EXPRESS

12. A. Carena, G. Bosco, V. Curri, Y. Jiang, P. Poggiolini, and F. Forghieri, "EGN model of non-linear fiber propagation," Opt. Express **22**(13), 16335–16362 (2014).
13. P. Serena and A. Bononi, "On the accuracy of the gaussian nonlinear model for dispersion-unmanaged coherent Links," in Proc. of European Conference on Optical Communications (ECOC), Th.1.D.3, ECOC (2013).
14. L. Galdino, G. Liga, G. Saavedra, D. Ives, R. Maher, A. Alvarado, S. Savory, R. Killey and P. Bayvel, "Experimental demonstration of modulation-dependent nonlinear interference in optical fibre communication," in Proc. of European Conference on Optical Communications (ECOC), P950 (2016).
15. P. W. Berenguer, M. Nöller, L. Molle, T. Raman A. Napoli, C. Schubert and J. K. Fischer, "Nonlinear digital predistortion of transmitter components," J. Lightwave Technol, Vol. 34, No. 8, pp. 1739–1745 (2016).
16. G. Khanna, B. Spinnler, S. Calabr and E.D. Man, "A memory polynomial based digital pre-distorter for high power transmitter components," in Proc. of Optical Fiber Communication Conference (OFC), M2C.4 (2017).

1. Introduction

Communication over optical fibre has become the underpinning technology of choice for global information systems. These systems have ever increasing throughputs to satisfy the demand for data that support new and growing services such as cloud computing and video-on-demand. Technologies used to meet this demand include wavelength division multiplexing (WDM), optical amplification and coherent detection. The success and widespread deployment of erbium doped fibre amplifiers (EDFAs) now presents a limitation to capacity growth, as the available gain bandwidth, over which WDM signals can be transmitted, is limited to approximately 5 THz for the conventional band (C-band) and 8 THz for the long band (L-band). Given this fixed bandwidth limit, one way to increase the transmission rates is to increase the system signal-to-noise ratio (SNR), and the spectral efficiency [1].

As is well known, the optical fibre channel is subject to Kerr nonlinearity; its refractive index depends on optical intensity, causing nonlinear phase shifts and the signal is distorted from the interaction between nonlinearity and amplified spontaneous emission noise, reducing the SNR. New techniques to increase the SNR in the presence of nonlinearity have been proposed such as digital back propagation [2], coded modulation schemes [1] or novel equalising strategies [3]. However, the question of how these techniques perform within a practical, fully loaded C-band transmission system needs to be answered for every case, and simply extrapolating is not reasonable.

Transmission experiments with bandwidths approaching the full C-band require an increase in the number of channels, which comes at the expense of more complex experimental implementation; the use of additional light sources and modulators to implement independent channels can require large banks of laser sources, modulators and schemes to overcome data correlation issues. An attractive alternative, due to its simplicity, is the use of spectrally shaped amplified spontaneous emission noise (SS-ASE) instead of independently modulated channels. This technique has been shown in [4, 5], and has been used in C-band experiments [3, 6–8] as well as extended L-band transmission [9].

As shown through extensive theoretical models the use of Gaussian noise gives a lower bound on system performance compared to modulated channels [10–12]. In the Gaussian noise (GN) model, the nonlinear distortions are represented as an additional noise term in the overall system signal-to-noise ratio, and referred to as nonlinear interference (NLI) noise [10]. Corrections for modulation format can be applied to the GN model to make what is termed the enhanced Gaussian noise (EGN) model [12], which addresses the non Gaussianity of the signals. These models can be used to estimate the expected performance from using SS-ASE and modulated channels as interferers.

In this paper we evaluate the use of SS-ASE as a channel loading scheme compared to modulated interferers and quantify the effect of the additional NLI noise from this scheme on 4QAM and 64QAM modulated channels. The EGN model was used to verify the experimental results. Advanced transmission systems operating at 400 Gb/s and higher use coded modulation to

Optics EXPRESS

achieve the required high spectral efficiencies hence the penalty in terms of mutual information (MI) was also investigated as a function of distance. This enabled the impact of SS-ASE as a loading source to be quantified in terms of achievable information rate.

2. Modelling the NLI from SS-ASE

Research on the nonlinear fibre channel has led to various mathematical models to predict the NLI and hence the received SNR, which is used in system design and achievable rate estimations. These models use analytical expressions to provide a theoretical understanding of the experimental phenomena being investigated. A commonly used model due to its simplicity is the GN model [10]. This model has limitations as it assumes the CUT and interfering channels are made up of Gaussian noise (spectrally shaped as the actual channels) or, equivalently, by channels modulated by a Gaussian constellation. To properly account for non-Gaussian modulation formats, such as QAM, corrections have been applied to obtain the EGN model [12], which is used here. To confirm experimental results with the different schemes of interferers the GN and EGN models were used together to estimate the amount of NLI and hence the SNR of the channel under test (CUT).

The received SNR can be expressed as [7],

$$SNR = \frac{P}{\eta P^3 + \kappa P + N P_{\mathrm{ASE}}}, \tag{1}$$

with signal power P, the number of spans N, the nonlinear interference (NLI) coefficient for the entire link η and the ASE noise power from each amplifier P_{ASE}. The transceiver $\mathrm{SNR}_{\mathrm{TR}} = 1/\kappa$ is the maximum SNR that can be achieved in the transmission system in the absence of NLI and ASE noise. This variable phenomenologically includes all impairments of the system under test and can be measured in a back-to-back configuration without ASE noise loading. In this work, a $\mathrm{SNR}_{\mathrm{TR}}$ of 20.1 dB was measured. The NLI coefficient η includes contributions from self phase modulation, cross phase modulation and four-wave mixing [12].

It has already been shown that the input distributions of the transmitted channels affect the amount of NLI [13] and verified experimentally [14]. It has been shown that the amount of additional NLI is proportional to 4th standardized moment (kurtosis). The excess kurtosis of a complex random variable (kurtosis minus 2) such as a QPSK modulated signal is -1, whilst for SS-ASE it is 0. The higher the kurtosis the larger the nonlinear distortion [13].

The EGN model was used to estimate the performance of the channel under test with modulated channels as interferers. The correction from [12] is applied for self channel interference (SCI), multi channel interference (MCI) and cross channel interference (XCI) accounting for the modulation format dependence of the NLI noise. When using SS-ASE as an interfering channel, the EGN model is used to calculate the self channel interference but the correction for XCI and MCI are not applied. This corresponds to the GN model being used for interferers. That is the NLI coefficient for all channels (η_{chans}) and SS-ASE ($\eta_{\mathrm{SS\text{-}ASE}}$) are calculated as follows,

$$\eta_{\mathrm{chans}} = \eta_{SCI}^{GN} + \eta_{SCI}^{corr} + \eta_{XCI}^{GN} + \eta_{XCI}^{corr} + \eta_{MCI}^{GN} + \eta_{MCI}^{corr}, \tag{2}$$

$$\eta_{\mathrm{SS\text{-}ASE}} = \eta_{SCI}^{GN} + \eta_{SCI}^{corr} + \eta_{XCI}^{GN} + \eta_{MCI}^{GN}, \tag{3}$$

where η_{SCI}^{GN}, η_{XCI}^{GN} and η_{MCI}^{GN}, are the NLI coefficient contributions from the Gaussian noise model for self channel interference (SCI), cross channel interference (XCI) and multi channel interference (MCI) respectively and η_{SCI}^{corr}, η_{XCI}^{corr} and η_{MCI}^{corr} are the NLI coefficient corrections from the EGN model for SCI, XCI and MCI respectively. This is shown diagrammatically as optical spectra in Fig. 1. The additional η_{XCI}^{corr} contributions that have modulation format dependence of the CUT itself have been neglected.

Optics EXPRESS

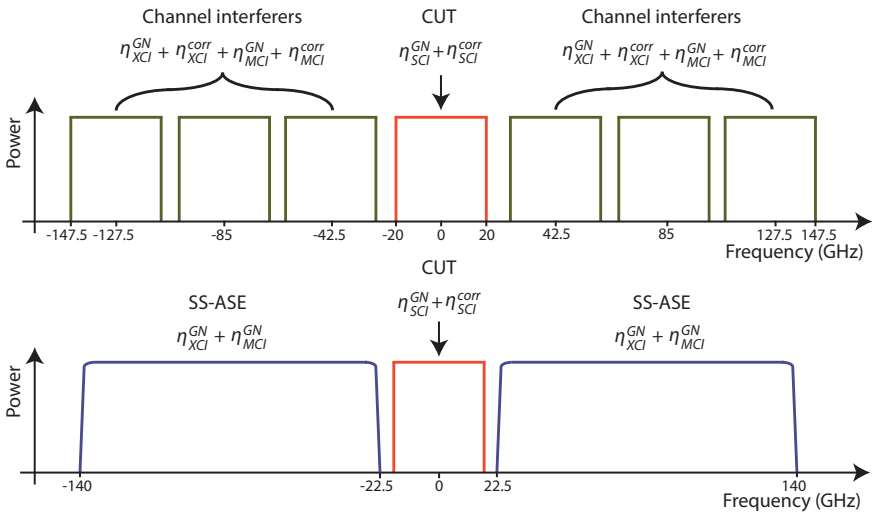

Fig. 1. Diagrammatic setup showing the optical spectra for two different interfering schemes for the channel under test (CUT). Top, 6 channels carrying modulated data and bottom, spectrally shaped ASE with the same occupied bandwidth

The modelling of SS-ASE in this paper is carried out by assuming that the spectral density is uniform. This is unlike the case of channel interferers in which guardbands are placed between each channel. In order to control this issue the total occupied bandwidth was maintained.

In order to compare the model with the experimental results, the linear impairment from ASE noise (P_{ASE}), transceiver noise $\mathrm{SNR}_{\mathrm{TR}}$, EDFA noise figures, recirculating loop losses and the fibre's dispersion and attenuation parameters were matched.

3. Experimental setup

The experimental setup used to quantify the effects of using SS-ASE in terms of SNR and achievable rate is shown in Fig. 2. The transmitter consisted of two sections, namely the SS-ASE source and the digital transmitter. The SS-ASE source was designed as follows: an ASE noise source was launched into an EDFA with an output power of 27 dBm, followed by a wavelength selective switch (WSS). The WSS cut a notch into the ASE with a width of 43 GHz centred on the carrier frequency of the CUT, with an extinction ratio of 35 dB. The WSS was used to limit the total bandwidth of the ASE noise source to 240 GHz and flatten the spectral profile by attenuating the wavelengths as necessary, in order to emulate the Nyquist spaced channels as shown in Fig. 1. To evaluate the performance of the system using SS-ASE all the ECLs at the transmitter, with exception of the CUT, were switched off, allowing the coupling of the CUT with the SS-ASE. The performance of channel interferers was evaluated by using all 7 ECLs and switching off the SS-ASE source, allowing transmission of the modulated channels.

The digital transmitter was constructed as follows. The drive signals were generated from a sequence of random data 2^{16} bits long before being mapped to either 4QAM or 64QAM symbols, as required for multiformat comparisons. These digital signals were then nonlinearly pre-emphasised using a Volterra filter to compensate for the non-ideal transmitter components [15,16]. The symbol rate was set to 40 GBaud and then a root raised cosine filter with a rolloff of 0.1% was applied. These 40 GBaud signals were uploaded to 92 GSa/s DACs and were linearly amplified before going into 2 separate IQ modulators. Two groups, one of 4 and one of 3 ECLs, with 100 kHz nominal linewidth, were passed into the single polarisation modulators such that independent odd and even modulation patterns were obtained. The spacing of the lasers was set

Optics EXPRESS

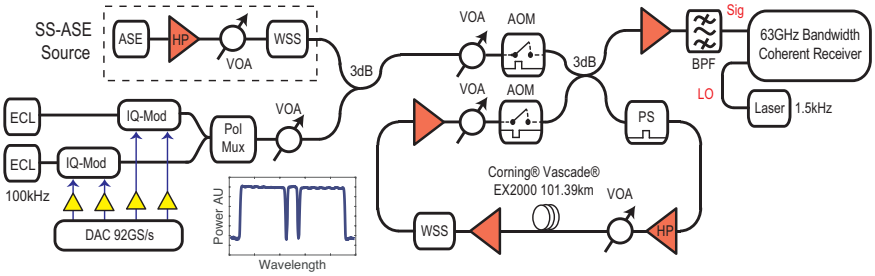

Fig. 2. Experimental Setup, showing the SS-ASE source constructed from an ASE source, high power (HP) EDFA, variable optical attenutator and wavelength selective switch (WSS), the digital transmitter using external cavity lasers (ECLs), polarisaiton multiplexer (Pol. Mux.) and IQ modulators (IQ Mod.), and a recirculating loop using acousto-optic modulators(AOMs), polarisation scrambler (PS) and WSS for gain flattening and a band pass filter just before the coherent receiver. Inset, optical spectrum showing one channel with 240 GHz of SS-ASE.

at 42.5 GHz. The output of the modulators went into a polarisation multiplexing emulator in order to generate polarisation division multiplexed signals.

The output of the digital transmitter was then combined with the SS-ASE source using a 3 dB coupler. The power spectral density of the SS-ASE noise and the transmitter were matched to within 0.3 dB. The power of the combined signal was measured using an optical spectrum analyzer with a resolution of 0.1 nm. This enables emulation of a re-configurable number of SS-ASE channels with arbitrary spacing and bandwidth with an improved performance compared to that reported in [5]. The extinction from the stop band to pass band was 35 dB and an EDFA with higher output power of 33 dBm allowed a larger ASE bandwidth to be filled whilst maintaining a constant power spectral density.

For transmission, a recirculating loop was used, with a loop-synchronous polarization scrambler (PS), and a single span of 101.39 km of Corning® Vascade® EX2000 fiber with a total loss of 16.2 dB. The span was followed by an EDFA with 18 dBm output power and 5 dB noise figure to overcome fiber attenuation. This was followed by another WSS which was used as a programmable gain flattening filter to compensate gain tilt from the optical amplifiers, followed by another EDFA in order to overcome the remaining component losses. An ECL with 12 dBm output power and 1.5 kHz nominal linewidth was used as the local oscillator in the coherent optical receiver. Detection was carried out using balanced photodetectors with an electrical bandwidth of 70 GHz (optical bandwidth 140 GHz). The received signals were captured by a real-time digital oscilloscope with an analog electrical bandwidth of 63 GHz (optical bandwidth 126 GHz) at 160 GSa/s. The symbol rate and spacing is such that 3 channels can be simultaneously captured.

The captured traces were processed offline, applying the following DSP chain. A correction for IQ delay in the receiver was applied, followed by ideally compensated chromatic dispersion. The signal was then root raised cosine filtered before equalisation. This was performed by using a constant modulus algorithm to preconverge taps for a least mean squares radially directed equaliser. The frequency offset between carrier and LO was then estimated before a decision directed algorithm was used for carrier phase estimation. Gram-Schmitt orthogonalisation was finally performed to compensate for sub-optimal phase biasing of the transmitter IQ modulators. Decisions were then made on the symbols and compared to the ones that were sent to generate a bit error rate and calculate SNR. Then MI was calculated over both polarisations, on the sent and received symbols for the experiment and for the model as a function of the measured SNR and modulation format; details of the MI calculations are in [1].

Optics EXPRESS

4. Experimental and theoretical transmission results

The channel under test was modulated with either 4QAM or 64QAM data and propagated over 20 recirculating fibre loop spans, with a total distance of 2028 km. For bandwidth loading two schemes were used, with channels either carrying the same modulation format as the CUT or loaded to the same bandwidth of 282.5 GHz with SS-ASE, from here on referred to as channel interferers and SS-ASE respectively. The results from sweeping the launch power, the transmission distance and varying the total transmission bandwidth are shown below.

4.1. Launch power investigation

The received SNR was experimentally measured for launch powers in the range -5 to +7 dBm per channel, and is shown in Fig. 3 a) and Fig. 4 a) for 4QAM and 64QAM respectively. For modeling channel interferers using the EGN, a channel spacing of 42.5 GHz was used. For SS-ASE a flat spectral density was assumed and the width of the CUT was taken as 42.5 GHz, which includes the guardband. Considering the remaining guardbands, the SS-ASE bandwidth was limited to that occupied by the channels not including the guardband i.e. 240 GHz. It can be seen that for both schemes of interfering channels the performance of the CUT at low launch powers is identical. This is due to the main source of noise being P_{ASE} from the EDFAs. As the launch power is increased the performance of the CUT is affected by NLI noise and the performance achieves a maximum and then starts to decrease.

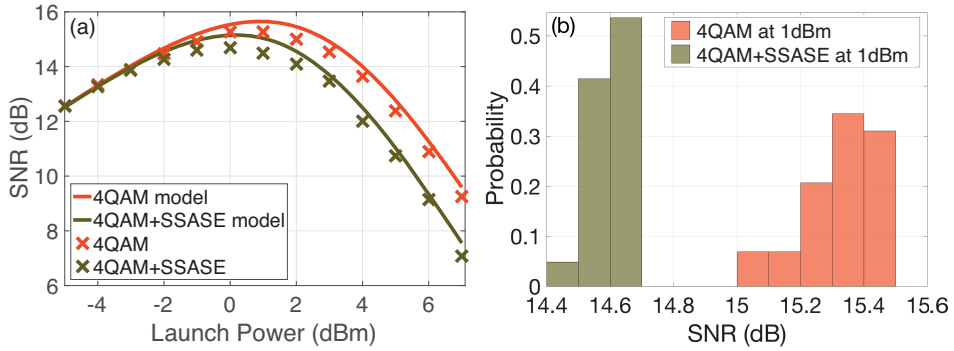

Fig. 3. a) SNR as a function of launch power for just channel interferers and 1 channel with SS-ASE taken at 2048 km. Crosses are experimental points and solid lines are the model b) Histogram of SNR of the CUT over time for channel interferers and SS-ASE for 4QAM at a fixed launch power of 1 dBm.

In Fig. 3 a), it can be seen that the predicted SNR of the model agrees with the experimental data to within 0.5 dB. It can also be seen that when the bandwidth loading was SS-ASE, the peak SNR is lower and hence the NLI is higher compared to that of channel interferers. In order to quantify the effects of the additional NLI from SS-ASE, the optimum experimental SNR for both schemes was found. This was estimated by fitting a third order polynomial to the data using a LSE approach and taking the maximum of that polynomial.

For 4QAM channel interferers the maximum SNR was 15.19±0.10 dB and for SS-ASE 14.62±0.13 dB with corresponding optimum launch powers of -0.2 dBm and 0.8 dBm. The confidence interval of 50% is calculated from the errors between the data and the assumed cubic polynomial. The change in peak SNR between the two cases is 0.57±0.16 dB and was predicted to be 0.50 dB by the model. In order to be sure of this change in SNR the launch power was fixed at 1 dBm and multiple readings were taken for both interferer schemes over time and plotted in a histogram as shown in Fig. 3 b). This is 0.2 dBm lower than optimum

Optics EXPRESS

launch power for the 4QAM CUT with 4QAM interferers and 1.2 dB higher than optimum for SS-ASE. At this launch power the delta in SNR between the two bandwidth loading schemes is larger so is more visible experimentally. 50 samples were taken for each scheme. From Fig. 3 b) it can be seen that the penalty in SNR (difference in means) is 0.72 dB with a standard deviation of σ=0.13, with the model predicting 0.61 dB. This agreement within error between experiment and model shows that the use of SS-ASE as a replacement for channel interferers gives a pessimistic evaluation of performance.

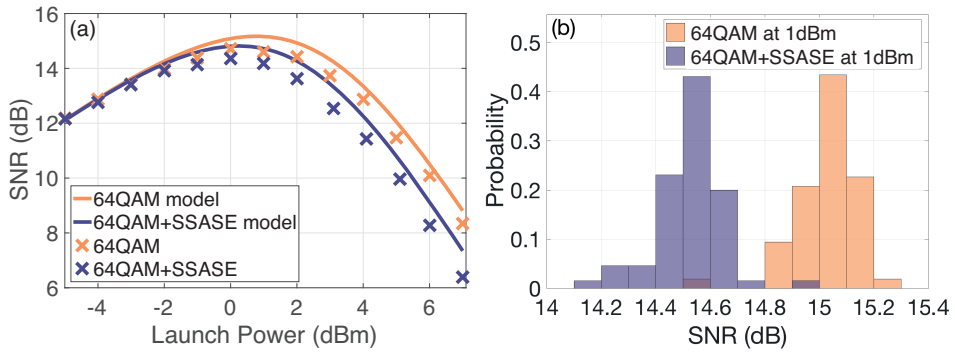

Fig. 4. a) SNR as a function of launch power for just channel interferers and 1 channel with SS-ASE taken at 2048 km. b) Histogram of SNR of the CUT over time for channel interferers and SS-ASE for 64QAM at a fixed launch power of 1 dBm.

The results of the power sweep for 64QAM with both schemes of interfering channels are shown in Fig. 4. The difference in peak SNR from 64QAM to SS-ASE is 0.40 dB. The SNR of the CUT was again taken over time for both schemes at a fixed launch power of 1 dBm per channel. Again, 50 samples were taken for each scheme. The resulting offset in mean SNR was 0.49 dB with a standard deviation of σ=0.11. This difference in SNR at optimum and in the nonlinear regime is smaller than that of 4QAM and agrees with the predictions made by the model of 0.37 dB at optimum and 0.44 dB at 1 dBm.

This corroborates with the fact that the modulation format of the interfering channel affects the amount of nonlinear interference noise on the CUT. Here SS-ASE can be thought of as Gaussian modulation. This has an excess kurtosis of 0, which is greater than the values of -1 and -0.62 for 4QAM and 64QAM channels respectively.

4.2. *Distance investigation*

This subsection investigates the system performance as a function of distance when replacing channel interferers with SS-ASE. The mutual information (MI) of the CUT as a function of distance (100 km to 2500 km) is shown in Fig. 5. A launch power of 2 dBm per channel was chosen in order to more clearly show the difference in performance between interfering schemes. As can be seen at shorter distances the MI drops slowly and to up to 300 km, the SS-ASE and channel interferers have the same performance. At shorter distances, the transceiver $\mathrm{SNR}_{\mathrm{TR}}$ (which sets the highest MI in the system) is the predominate source of noise in the system. For longer distances, the effect of $\mathrm{SNR}_{\mathrm{TR}}$ becomes less significant, and the system performance is dominated by accumulation of ASE and by NLI. For instance, at 2000 km the channel interferers outperformed the SS-ASE by 0.43 b/sym. It can also be observed, the difference between the model and experimental results as the distance increases is due to the WSS being reprogrammed for each change in the number of recirculations to maintain spectral flatness. The additional nonlinear distortion incurred from the SS-ASE can be seen to affect the performance significantly beyond 800 km. This is the regime in which NLI noise forms a significant contribution of the

Optics EXPRESS

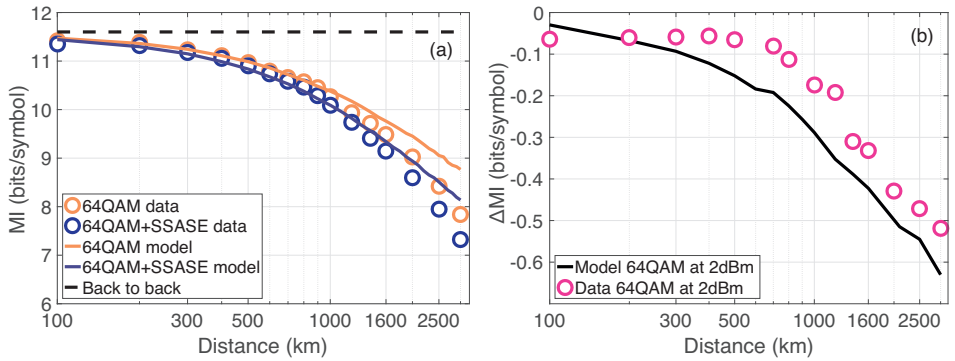

Fig. 5. Mutual information (MI) shown as a function of distance for both schemes. Markers are experimental points taken at a fixed launch power and lines are from the model. a) channel interferers (orange) and SS-ASE (purple). b) shows the difference in MI between channel interferers and SS-ASE as a function of distance

total noise compared to the transceiver noise. Hence, the previous launch power curves were taken at 2000 km to demonstrate the NLI independent of transceiver limits.

The change in MI from both interfering channels being either 64QAM or SS-ASE as a function of distance is shown in Fig. 5 b). The discontinuous nature that can be seen in the model results is due to errors in the Monte-Carlo integration used to calculate the η in equation 1. The same trend can be seen in ΔMI, that the transceiver noise affects the distance at which NLI becomes significant. Once out of the transceiver limit this difference is seen to increase. The measured offset from channel interferers and SS-ASE in SNR is 0.8 dB at 2000 km, corresponding to a change in MI of 0.4 bits/sym which is 5% of the achievable rate.

The penalty after 800 km of transmission corresponds to a decrease in MI of 0.07 bits, a change in capacity of 0.6%. The difference in SNR at optimum launch power is smaller than that shown at 2 dBm, so the measured Δ MI in Fig. 5 b) is larger than would be expected at optimum launch power. This means when evaluating SNR at short distances with optimum launch power, close to where transceiver noise is dominant, using SS-ASE as an interfering channel is a very reliable estimate of performance as the penalty is less than 0.6%. The difference in SNR and MI between channel interferers and SS-ASE, is noted to always be negative, so the SS-ASE will always give a pessimistic prediction of the impact of NLI on system performance.

4.3. *Bandwidth investigation*

In order to investigate the implications of using SS-ASE as a replacement of channel interferers beyond the experimental transmission bandwidth of this work, we extended the study of system performance for bandwidths up to 4.5 THz using the theoretical model. The system under consideration has a fixed transmission distance of 2000 km and 40 GBd modulated channels carrying dual polarisation 64QAM. Fig. 6 shows the difference in SNR at optimum signal launch power between the use of channel interferers, and SS-ASE as a function of total transmission bandwidth. Each line represents a different number of channel interferers (adjacent to the CUT) out of the total transmission bandwidth. It can be seen that as the total transmission bandwidth increases, a larger penalty in SNR is observed when SS-ASE is used instead of channel interferers. This is due to the logarithmic growth of the nonlinear distortions as a function of bandwidth, as seen in [9, 10]. It is noted that when a single modulated channel is propagated with SS-ASE to fill the full C-band, a penalty of 0.8 dB is observed, however if seven modulated channels are propagated together with SS-ASE this penalty is reduced to 0.6 dB. The use of a higher number of channel interferers before employing SS-ASE decreases the penalty from nonlinear

Optics EXPRESS

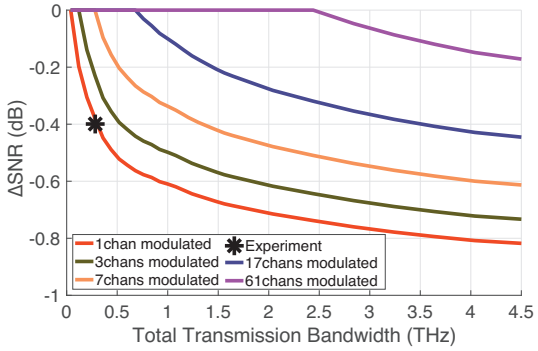

Fig. 6. Difference in peak SNR between channel interferers and SS-ASE as a function of bandwidth for different number of channel interferers at optimum launch power. For a transceiver with a maximum SNR of 20.1 dB at 2000 km. The marker is the experimental work conducted in this paper.

distortions. This is because the higher NLI generating SS-ASE is spectrally further away from the CUT. This shows that using SS-ASE to load the fibre will provide a useful estimate of performance. In the worst case for this system of a fully loaded C-band, the replacement of channel interferers with SS-ASE only gives a penalty of 0.8 dB.

5. Conclusion

The use of SS-ASE loading in the design and evaluation of wideband (up to a full C-band) optical fibre transmission systems was investigated in detail for the first time. It was shown that SS-ASE generates additional nonlinear interference noise, compared to that of conventional channel based interferers. The described model in this paper treats SS-ASE as Gaussian modulation, which gives an accurate method to predict performance. The NLI from SS-ASE is larger than that from 64QAM interferers, and even larger than 4QAM interferers. The increase in NLI noise reduces the SNR and hence SS-ASE always gives an underestimate. There is good agreement between the model and experimental results which highlight that the conservative or pessimistic estimate through using SS-ASE as an interferer is the same as the underestimate that comes from using the GN model with out corrections. The change in MI was calculated to understand the effect of SS-ASE in systems that use coded modulation. It was shown that the change in MI at the optimum launch power for this scheme was 0.6% of the achievable rate at 800 km and 5% at 2000 km and the measurements confirmed that using SS-ASE as a method of loading a fibre provides a pessimistic estimate on system performance. The greater the number of channel interferers used before SS-ASE is employed, the smaller the penalty. Using SS-ASE to load 4.5 THz of bandwidth when using one modulated channel only gives a reduction of 0.8 dB in SNR. If a total of 17 modulated channels (representing 15% of the total 4.5 THz) are used, the SNR is reduced by only 0.42 dB, making SS-ASE an invaluable tool for the design and verification of fully loaded, wideband transmission systems.

Funding

U.K. Engineering and Physical Sciences Research Council (EPSRC) under Grant EP/J017582/1 (UNLOC), INSIGHT and EPSRC iCASE award with the BBC.